Available online at www.sciencedirect.com
ScienceDirect
Ceramics International 37 (2011) 2809–2820
CERAMICS INTERNATIONAL
www.elsevier.com/locate/ceramint

Factors affecting strength and shape retention of zirconia micro bending bars during thermal debinding

Fatih A. Çetinel *, Werner Bauer, Regina Knitter, Jürgen Haußelt

Karlsruhe Institute of Technology, Institute for Applied Materials (IAM-WPT), Hermann-von-Helmholtz-Platz 1, 76344 Eggenstein-Leopoldshafen, Germany

Received 15 March 2011; received in revised form 11 April 2011; accepted 26 April 2011
Available online 4 May 2011

Abstract

Low-pressure injection moulded (LPIM) zirconia (3Y-TZP) micro bending bars with bending strength up to 2808 MPa were fabricated. It was found that an increase of the surfactant concentration of the processed feedstocks results in an improvement of surface finish and strength of sintered micro bending bars. During thermal debinding, the formation of a binder film on the surface of the micro parts could be observed, which is responsible for the healing of surface defects. Due to high surface-to-volume ratio surface defects determine the fracture behaviour. Thus, the mechanical properties are improved, if the number and size of surface defects and the surface roughness of the micro bending bars can be reduced. However, an improvement of the surface quality is usually associated with rounding of edges and, in the worst case, the loss of geometrical integrity. Several material and process-related factors were found to influence shape retention and, as a result, surface quality and strength of LPIM ceramic micro parts during the binder removal. To ensure a reproducible fabrication it is necessary to control all material and process-related factors. In this study an interesting opportunity for an in-process improvement of the strength of ceramic micro parts is presented.

Keywords: Low-pressure injection moulding; 3Y-TZP; Surface defects; Surface finish

1. Introduction

Due to the growth of microsystem technology (MST) and the rising need for miniaturization of technical devices, the interest in powder injection moulding of micro components (μ-PIM) has increased in the last years [1]. Besides polymers and metals, ceramic materials are attaining more importance in modern technology, since they combine unique properties, such as outstandingly good mechanical, chemical, thermal, tribological and other special physical properties [2]. High precision parts for dental and medical applications, such as orthodontic brackets and small surgical forceps and scissors, as well as components for microelectronics, such as fibre optic connectors and semiconductor wire bonding tools, are examples for ceramic micro components [3]. Plastic shaping techniques, in particular μ-PIM, enable near net shape fabrication of complex shaped ceramic micro components. Considering an increasing demand for customized ceramic micro parts and components [4], low-pressure injection moulding (LPIM), which is sometimes also referred as hot moulding [5], is a predestined fabrication method for prototypes and small series, as cost-effective and re-useable moulds can be used [6,7]. By applying rapid prototyping process chain (RPPC) techniques [2,8], fast and inexpensive manufacturing of ceramic parts down to the micron range can be realized via LPIM, which was recently demonstrated in a successful case study on a ceramic micro turbine [9].

Feedstocks for LPIM require good mouldability and sufficiently high resistance of green parts to deformation during thermal debinding. On the one hand, a low feedstock viscosity and a low yield point are necessary to enable complete mould filling even at low moulding pressures. On the other hand, a high viscosity and high yield point are needed to ensure shape retention during the binder removal step [4]. One major drawback of LPIM is the poor mechanical strength of green parts during thermal debinding. For LPIM, low feedstock viscosity and yield point are required to enable mouldability at low pressures. Therefore, backbone polymers, which are

* Corresponding author. Tel.: +49 721 6082 4055; fax: +49 721 6082 4612.
E-mail address: fatih.cetinel@kit.edu (F.A. Çetinel).

0272-8842/$36.00
doi:10.1016/j.ceramint.2011.04.076

commonly used for high-pressure injection moulding (HPIM), cannot be used as binders for LPIM. The application of backbone polymers, such as polyethylene, results in enhanced mechanical strength of green parts during debinding. However, as the feedstock viscosity and yield point are significantly increased, high injection pressures are required for moulding. Furthermore, as the LPIM binder systems usually consist of paraffin wax and a surface active agent (surfactant) only, such binder systems melt over a narrow temperature range, where the green part becomes soft and deformable. Thus, for thermal debinding of LPIM green parts defect free binder removal is generally more complicated than for HPIM parts.

However, it is possible to turn these drawbacks of LPIM into a chance for improving the reliability of ceramic micro components. Dense microstructures and a sufficiently high surface-to-volume ratio are a prerequisite to enable a micro-specific feature of the thermal debinding of LPIM ceramic micro parts. In this case, the fracture behaviour is determined by surface defects. At the initial stage of debinding (70–150 °C), levelling and healing of surface defects occur due to the formation of a distinctive surface binder film on the micro parts. Hence, the surface tension of the binder in connection with a reduction of binder viscosity as well as the yield point of the feedstock formulation result in an improvement of the surface quality and strength of the micro parts. However, this improvement is usually associated with rounding of edges and, in the worst case, the loss of geometrical integrity of the micro part.

The aim of this study is to contribute to a precise understanding and control of the micro-specific processes during the binder removal in order to retain the parts' shape and to improve the mechanical properties. Several material and process-related factors influencing the shape retention of green parts during debinding and, as a result, the surface quality and strength of sintered zirconia micro bending bars are presented. The knowledge and ability to control a number of material and process-related factors makes it possible to ensure a reproducible fabrication of hot moulded ceramic micro parts with improved mechanical properties.

2. Experimental

Feedstocks were prepared using zirconia powder containing 3 mol% Y_2O_3 (TZ-3YS-E, Tosoh, Japan) with an average particle size of 390 nm and a specific surface area of 6.6 m^2/g. Binder formulations were based on paraffin wax (TerHell Paraffin wax 6403, Schümann Sasol, Germany) with a setting point at 64.5 °C, and a commercial surfactant (Hypermer LP1, Croda, UK). Solids loadings of the feedstocks were kept constant at 50 vol%, whereas the amount of the surfactant was varied from 1.6 mg/m^2 to 3.2 mg/m^2. The powder-binder mixture was plastified and homogenized at standard working temperature of 90 °C using a laboratory vacuum dissolver (Dispermat, VMA-Getzmann, Germany).

Micro bending bars were prepared by applying a rapid prototyping process chain (RPPC) [2,8]. An array of 15 × 15 columns with square cross section, manufactured via micro milling of brass, was used as a master model for the casting of silicone moulds (Fig. 1), which were used, in turn, for replication by applying a manual option of the LPIM process. Feedstocks at standard working temperature were moulded manually into the preheated silicone moulds and evacuated under vibration. This pressureless mould filling technique is possible due to the low viscosity of the feedstocks. It was favoured over a semi-automatic LPIM machine, as the required feedstock amount is considerably smaller than using a machine, so that it is more suitable in laboratory scale. Moulding times (filling of mould and evacuation) varied from 2 min to 30 min. After moulding and evacuation the feedstock was cooled down in the silicone mould at ambient air. Demoulded green parts

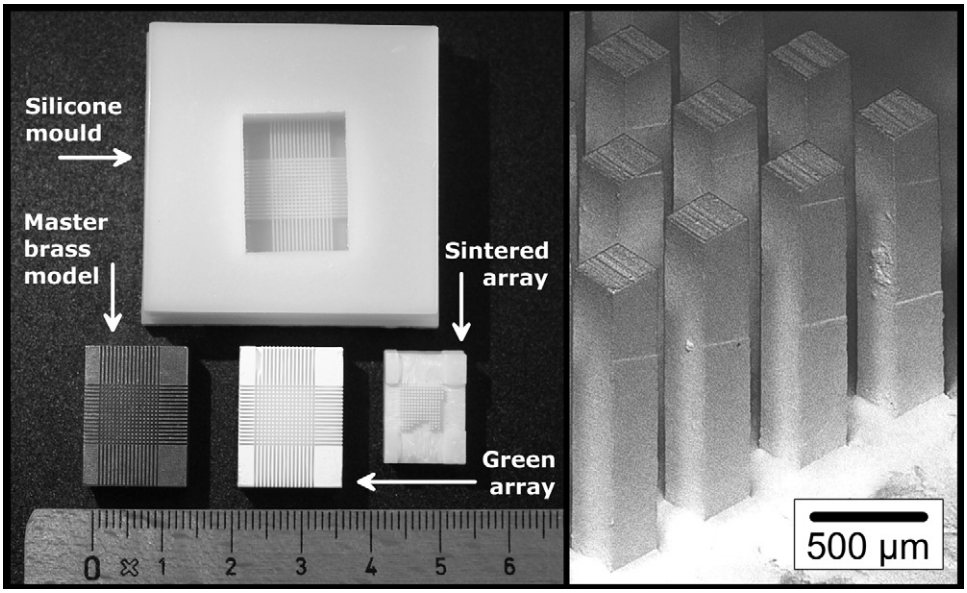

Fig. 1. Illustrations of the silicone mould, brass master model, green array, sintered array (left) and light-optical microscope micrograph of thermally debinded micro bending bars (right).

were stored in an exsiccator or debinded immediately. Thermal debinding of the green column arrays was conducted on porous alumina plates (Keralpor 99, Kerafol, Germany) at 500 °C using a debinding furnace with air circulation (HT6/28, Carbolite, UK). Pressureless sintering in air was performed with 3 K/min up to 1450 °C and a dwell time of 60 min (VMK1800, Linn High Term, Germany). The columns exhibit dimensions of about 250 μm × 250 μm × 1500 μm in the green state and approximately 200 μm × 200 μm × 1200 μm after sintering.

Characteristic strength and Weibull modulus of a set of 30 bending bars per array were evaluated according to EN 843-5 [10] using a self-designed micro 3-point-bending device with an outer span length of 800 μm [11]. The testing jig was developed at the Institute for Applied Materials (IAM-WK) of the Karlsruhe Institute of Technology (formerly Institute of Materials Science and Engineering I of the University of Karlsruhe) [12]. While loading, subcritical crack growth could be avoided, as a movement speed of 2 μm/s of the lower support was applied, which resulted in a minimum loading rate of 400 MPa/s. To prevent measurement inaccuracies at incipient loading, the samples were fixed by applying a pre-load of 2 N. An edge guide fixture was used to enable a centred and parallel positioning of the samples on the lower supports to avoid measurement inaccuracies due to tipping or incorrect alignment of the micro bending bars. By reason of the small dimensions, only static supports could be used, which were fabricated via wire-electro discharge machining of a hard metal exhibiting an edge radius of 50 μm and 100 μm for the lower and upper supports, respectively. Considering the standard deviation of random errors, as measurement of width and height of the samples' cross-sections and the deviation of the signal repeat accuracy of the load cell [13], a relative error of maximum 2% of the bending strength was calculated. As friction at the sample-loading point interface may largely affect the measured values, it gives rise to an increase of the apparent strength [14–17]. Considering a coefficient of friction of 0.3 for the tribosystem 3Y-TZP against hard metal at ambient conditions [18] and the fact that friction is minor for 3-point bending compared to 4-point bending, the overestimation of the bending strength due to friction was calculated to be not higher than 9% [14].

Measurements of sintered density were conducted according to the Archimedes' method. Relative sintered density values are based on a theoretical density value of 6.09 g/cm^3 for 3Y-TZP [19,20]. The averaged roughness height R_Z (DIN 4768) [21] of sintered micro bending bars was determined using a non-destructive metrological surface measuring system (MicroProf, Fries Research & Technology FRT, Germany) with chromatic white light sensor. A digital light microscope (VHX 500F, Keyence, Japan) was used for analysis of green parts and fracture surface of sintered bending bars as well as the measurement of geometrical dimensions. A minimum inherent edge rounding of 2–3 μm of the sintered micro parts was considered to be due to the micro-milled brass master model. Rheological properties of feedstock and binder formulations were determined using a rotational rheometer (MCR 300, Anton-Paar, Austria). Real-time observations of the thermal debinding process were conducted using a video-based optical contact angle meter (OCA20, DataPhysics Instruments, Germany). Thermogravimetric analysis (STA 449 C Jupiter, Netzsch, Germany) was carried out under air flow at a heating rate of 1 °C/min in the temperature range of 25–600 °C. Porosity values of powder compact and debinding support were determined according to the mercury intrusion porosimetry (Pascal 140, Porotec, Germany).

3. Results and discussion

3.1. Micro-specific characteristics of mechanical properties

Due to the probabilistic nature of the strength of ceramic components and its dependency on the specimen size [22], it is possible to predict the strength of ceramic parts with different sizes according to the well-known Weibull size-scaling relationship given in Eq. (1) (effective surface S_E and effective volume V_E are applied, if surface flaws and volume flaws are strength limiting, respectively). As fracture is caused by flaws distributed in the specimen, the probability of failure highly depends on the probability of finding a critical flaw in the ceramic component [14,23]. Therefore, presuming an invariant flaw type population, the strength of a small specimen can be predicted according to Eq. (1). As a result, the strength of a smaller specimen will be much higher than the strength of a specimen of bigger size. However, different flaw populations result in different strength distributions and, thus, yield in a different size-scaling [23,24], which was not the objective of the current study.

$$\frac{\sigma_{micro}}{\sigma_{macro}} = \left(\frac{S_{E,macro}}{S_{E,micro}}\right)^{1/m} \quad (1)$$

In the literature, 4-point bending strength values of about 600 MPa can be found for as-fired zirconia macro bending bars 3 mm × 4 mm × 48 mm with 3 mol% Y_2O_3 (3Y-TZP) [25]. Using Eq. (2) [26] this value can be transformed into a 3-point bending strength of about 700 MPa for a macro bending bar with similar geometry. In Eq. (2) σ_3 and σ_4 stand for the strength values of 3-point and 4-point bending configurations, respectively, L_3 and L_4 for the corresponding fixture span lengths and m for the Weibull modulus.

$$\sigma_3/\sigma_4 = \left(\frac{L_4}{L_3}\right)^{1/m}\left(\frac{m+2}{2}\right)^{1/m} \quad (2)$$

Applying the Weibull size-scaling relationship (Eq. (1)) using 700 MPa for as-fired strength of macro bending bars σ_{macro} and calculating the effective surfaces of $S_{E,macro}$ 3 mm × 4 mm × 30 mm [25] and $S_{E,micro}$ 0.2 mm × 0.2 mm × 0.8 mm for macro and micro bending bars [26], respectively, micro bending strength values σ_{micro} between 1202 MPa and 1575 MPa are predicted for varying Weibull moduli from 8 to 12 (Table 1). Presuming that volume

Table 1
Effective volume ($V_{E,micro}$) and surface ($S_{E,micro}$) of micro bending bars and results of the Weibull size-scaling from as-fired 3Y-TZP macro bending bars (3 mm × 4 mm × 30 mm) with 700 MPa to micro bending bars (0.2 mm × 0.2 mm × 0.8 mm).

Weibull's modulus m (–)	$V_{E,micro}$ (mm^3)	$S_{E,micro}$ (mm^2)	$\sigma_{micro,V}$[a] (MPa)	$\sigma_{micro,S}$[b] (MPa)	$S_{E,micro}/V_{E,micro}$ (–)	$S_{E,macro}/V_{E,macro}$ (–)
8	2.0×10^{-4}	2.0×10^{-2}	2246	1575	100	5.8
9	1.6×10^{-4}	1.8×10^{-2}	1973	1439	110	6.4
10	1.3×10^{-4}	1.6×10^{-2}	1779	1339	120	7.0
11	1.1×10^{-4}	1.4×10^{-2}	1634	1262	130	7.6
12	9.5×10^{-5}	1.3×10^{-2}	1523	1202	140	8.2

[a] Considering that volume defects are strength limiting.
[b] Considering that surface defects are strength limiting.

defects are strength limiting, values between 1523 MPa and 2246 MPa are predicted.

Irrespective of the Weibull's modulus, the surface-to-volume ratio of micro bending bars is always 17 times higher than the surface-to-volume ratio of macro bending bars (Table 2). Considering this, the fracture behaviour of micro bending bars is more likely to be affected by surface defects than by volume defects. Therefore, surface defects are seen as the strength limiting factor. In fact, the fracture surfaces of sintered micro bending bars show that solely surface defects like grooves, pores and flaws, originating on the tensile surface, are the reason for failure (Fig. 2). Micro bending bars made of feedstock formulations with surfactant concentration of 1.6 mg/m^2 and 2.0 mg/m^2 exhibit characteristic strength values in the range of the prediction from Eq. (1) (Table 2). However, strength values of samples fabricated with higher surfactant concentration (2.4 mg/m^2 and 3.2 mg/m^2) exceed this range, which is even more likely to be overestimated because of the very small specimen size, as the Weibull theory gets inconsistent for specimens having an effective volume of 10^{-4} mm^3 or less [27], which is valid for the micro bending bars used in this study (Table 1). Moreover, considering an effective moment of inertia of the sample's cross section due to the edge rounding, the strength is increased up to significantly higher effective strength values, e.g. $\sigma_{c,eff}$ of 2808 MPa for an edge rounding of 14.4 μm at 3.2 mg/m^2 surfactant concentration (Table 2). The influence of edge rounding on the sample's moment of inertia is discussed in detail elsewhere [28]. It is obvious that the Weibull size-scaling effect is one important reason for the high strength values obtained. However, it is not the only reason, as discussed later.

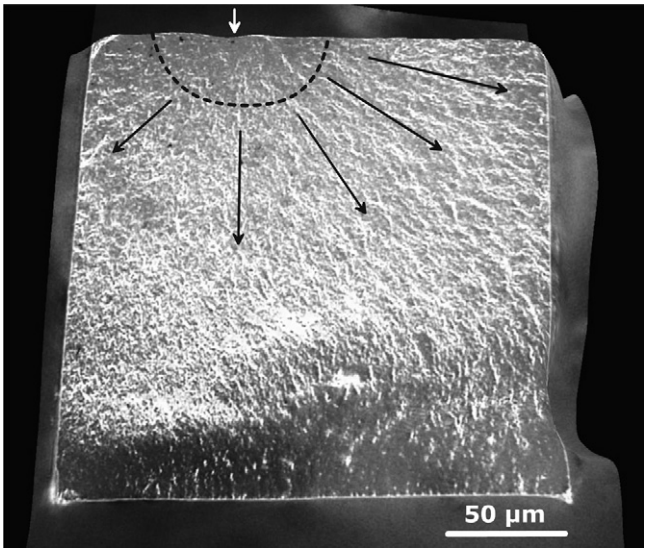

Fig. 2. Light-optical microscope micrograph of the fracture surface of a micro bending bar exhibiting an individual strength of 1628 MPa. Fracture occurred at the tensile surface (indicated by a downward arrow); the dashed line highlights the fracture; hackle lines are represented by arrows.

Sufficiently high relative sintering densities up to 99.6% of bulk arrays were measured (Table 2). As a pressureless variant of the hot moulding process was applied, the mould filling quality highly depends on the flowability of the feedstock. High viscosity values result in poor mouldability, what makes it difficult to remove entrapped air in the moulded feedstock completely and, thus, lower the sintering density of the bulk samples, as is evident from Table 2. However, the bulk density values below 99.6% should not be considered to represent the density of the micro parts. In fact, the sintering density of bulk samples with typical dimensions of about 16 mm × 12 mm × 6 mm is measured, which can be seen as a bulk substrate for the micro bending bars (Fig. 1). Irrespective of the feedstock flowability, the sintering densities of micro bending bars are supposed to be around 99.6%. Micrographs of the fracture surface (Fig. 2) and microstructure [29] as well as porosity measurements clearly show that neither volume defects nor porosity could be detected in the micro bending bars. Porosity values below 1% were measured in the sintered state.

3.2. Influence of material-related factors: surfactant concentration

In Fig. 3 the characteristic strength σ_c, surface roughness R_Z, and edge rounding r_{edge} of the micro bending bars are illustrated as a function of the surfactant concentration β_{surf} of the feedstock formulation. It is obvious that strength and edge rounding increase with increasing concentration of the surfactant, whereas the surface roughness decreases (Table 2).

For high surfactant concentrations levelling and healing of surface defects take place during thermal debinding. The number and size of surface defects decrease, which is obvious by a decrease of the surface roughness, resulting in an improvement of the bending strength (Table 2). Reduction of surface roughness and occurrence of edge rounding can be seen as an indication that defect levelling processes take place

Table 2
Characteristics of hot moulded zirconia micro bending bars.

Surfactant concentration β_{surf} (mg/m^2)	Weibull's modulus m (–)	Strength σ_c (MPa)	Roughness R_Z (μm)	Edge rounding r_{edge} (μm)	Strength[a] $\sigma_{c,eff}$ (MPa)	Viscosity[b] η (Pa s)	Sintered density[c] ρ_{rel} (%)
1.6	9.1	1148	3.7 ± 0.8	3.9 ± 0.7	1245	172	97.0
2.0	10.3	1417	3.0 ± 0.2	3.4 ± 0.6	1512	72	98.7
2.4	8.8	1895	1.3 ± 0.2	4.4 ± 0.6	2059	48	98.9
3.2	11.1	2235	0.9 ± 0.1	14.4 ± 1.3	2808	46	99.6

[a] Considering the effective moment of inertia of the sample's cross section due to rounding of the edges.
[b] Corresponding feedstock viscosity at standard working temperature of 90 °C (shear rate 10 s^{-1}).
[c] Relative sintered density of sintered bulk array based on a theoretical density of 6.09 g/cm$^{3.}$

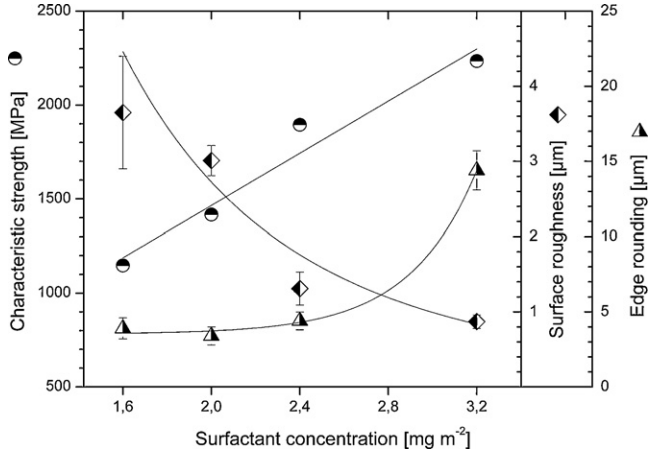

Fig. 3. Characteristic micro 3-point bending strength, surface roughness, and edge rounding of micro bending bars in dependency on the surfactant concentration of zirconia–paraffin wax feedstocks.

during thermal debinding. With increasing concentration of the surfactant enhancement of surface quality and occurrence of edge rounding of the micro bending bars are caused, which is the result of an interaction of several factors during the initial stage of the thermal debinding (70–150 °C):

(i) feedstock and binder viscosity,
(ii) yield point of the feedstock, and
(iii) surface tension of the binder.

In Fig. 4 the temperature dependencies of the yield point and the viscosity of a feedstock as well as the corresponding binder formulation are illustrated. A significant decrease of binder and feedstock viscosity can be observed from the melting point of the binder up to 130 °C. The yield point of the feedstock, which represents the rigidity of the particle network, also decreases in a similar way, which was already reported in a preliminary study [30]. Both, the decrease of binder viscosity and yield point of the feedstock, contribute to an enhancement of surface finish and an occurrence of edge rounding, as the mobility and rearrangement of particles on the surface of the bending bars are increased.

But the surface tension of the binder also plays an important part. It is well known that surfactants lower the surface tension of liquids. Thus, a reduction of the surface tension of paraffin wax is expected by adding the surfactant. As a result, higher edge rounding of the micro bending bars should be obtained at low surfactant concentrations, as high surface tensions are expected to enhance the driving force for rounding of sharp edges. In the Young equation (Eq. (3)) Δp stands for the pressure difference across the binder-to-ambient medium interface, γ for the surface tension of the binder and H for the mean curvature [31].

$$\Delta p = 2\gamma H \tag{3}$$

Contrary to expectations, the degree of edge rounding becomes higher for high amounts of surfactant (Table 2). Regarding the driving force for deformation and edge rounding, at low surfactant concentrations especially the high yield point of the feedstock seems to be more dominant than the surface tension of the binder. For instance, feedstock formulations with 1.6 mg/m^2 surfactant exhibit a yield point of about 460 Pa at 90 °C, whereas compositions with 2.4 mg/m^2 and 3.2 mg/m^2 show values of about 46 Pa and 7 Pa, respectively [30]. This remarkable decrease of the yield point results in a distinctive tendency for deformation. Initially, at high surfactant concentrations the effect of the surface tension of the binders starts to become effective and causes, in interaction with the low binder

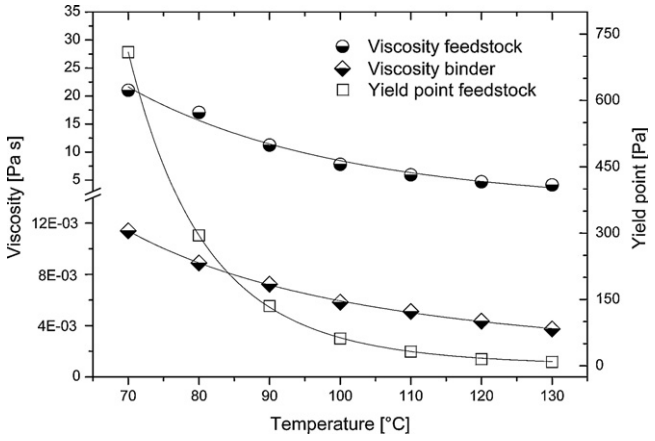

Fig. 4. Representative illustration of the temperature dependency of the yield point and viscosity of a feedstock and binder formulation with 2.0 mg/m^2 surfactant concentration (shear rate of 100 s^{-1}).

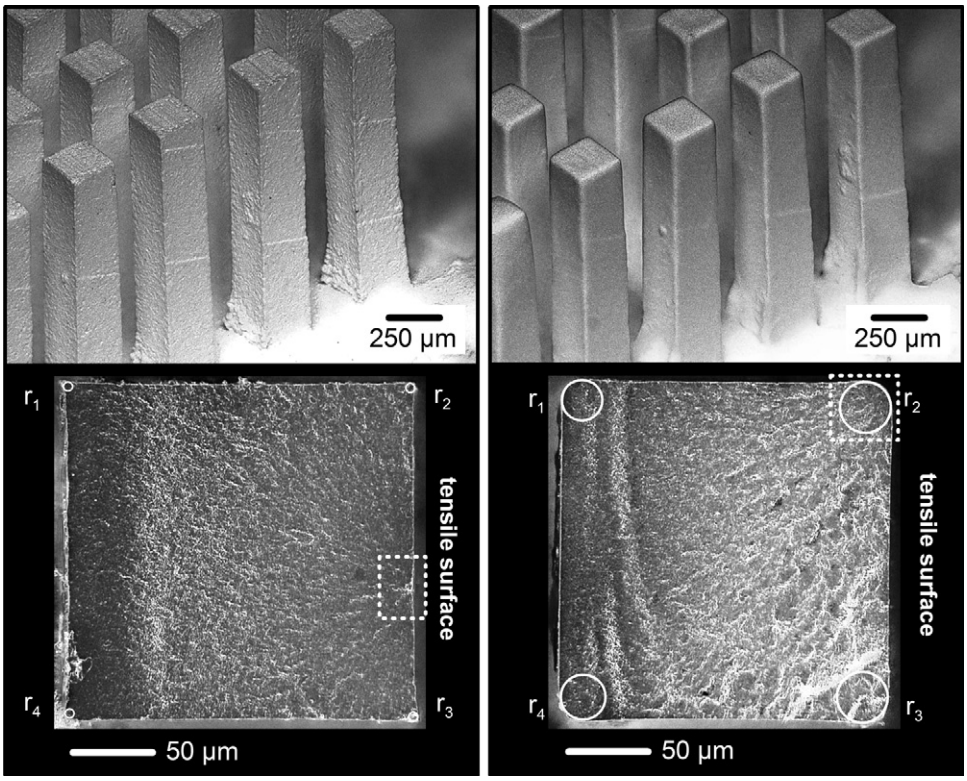

Fig. 5. Light-optical microscope micrographs of the surface of thermally debinded columns (top) and fracture mirror of sintered micro bending bars (bottom) fabricated of feedstocks with surfactant concentration of 1.6 mg/m^2 (left) and 3.2 mg/m^2 (right). Edge rounding diameter is represented by circles; the dashed rectangles highlight the fracture at the tensile surface.

viscosity and significantly reduced yield point, the occurrence of edge rounding.

Thus, the interaction of the decrease of binder and feedstock viscosity as well as the yield point of the feedstock and, additionally, the impact of surface tension of the binder altogether cause a micro-specific enhancement of the surface quality of micro bending bars. Depending on the amount of surfactant, this results in edge rounding at the initial stage of thermal debinding (Fig. 5). The improvement of surface finish and occurrence of edge rounding are seen as suitable indicators for the observed levelling and healing of surface defects. The decrease of the number and size of surface defects is evident by a reduction of the surface roughness and the enhanced mechanical properties of micro bending bars (Table 2). Besides the Weibull size-scale effect, it is obvious that the improvement of the surface quality of the micro bending bars is the major reason for the very high strength values obtained in this study.

3.3. Influence of process-related factors

3.3.1. Absorptivity of the debinding support

A distinctive binder film on the surface of low-pressure injection moulded micro bending bars was observed at the initial stage of debinding, which was already reported in a preliminary study [28] as well as in the literature [32,33]. In a recent study [34], similar observations were made during thermal debinding of LPIM alumina green parts. They were explained as an exudation effect due to the thermal expansion of the liquid binder in the initial debinding stage and described in terms of wick debinding of macroscopic green parts. The degree of binder exudation during debinding, however, is exceedingly crucial in the case of micro parts, as the geometrical integrity and the degree of edge rounding of the micro columns are affected significantly. According to Eq. (4) [35], a fraction w_{ex} of about 14% of the initial mass fraction of the binder w_b exudates at the melting point of the binder, generating the observed surface binder film. In Eq. (4) ρ_{bl} and ρ_{gd} stand for the density of the liquid binder and green part after debinding, respectively, and p for the porosity of the green part after debinding.

$$w_{ex} = 1 - p\frac{(1 - w_b)\rho_{bl}}{w_b\rho_{gd}} \quad (4)$$

By choosing a suitable debinding support, it is possible to retain the exudated surface binder film on the micro columns. In connection with a low yield point of the feedstock formulation either edge rounding or total deformation of the micro columns can be observed due to the effects discussed (Fig. 6a and b). The resistance against dimensional change is minor, since the binders used for LPIM feedstocks usually do not contain a backbone polymer that would hold the particles firmly together during debinding by sufficiently high binder and feedstock viscosity as well as high yield point of the feedstock. In contrast, the lack of a distinctive surface binder film up to temperatures, where the thermal degradation of the binder

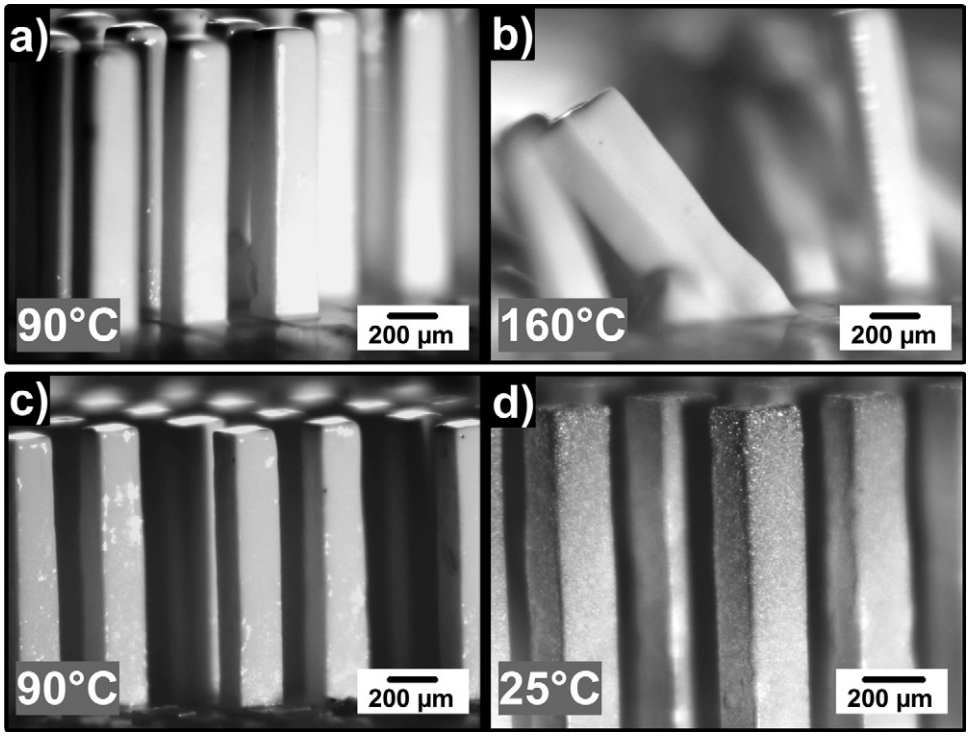

Fig. 6. Distinctive surface binder film for micro column arrays during debinding heating cycle at 90 °C (a), and total deformation at 160 °C (b) using a non-absorbing debinding support; by comparison, no distinctive surface binder film (c) and no deformation after cooling down (d) using an absorbing debinding support (heating cycle with 0.5 K/min up to 300 °C, feedstock formulation with 3.2 mg/m^2 surfactant).

starts, results in complete shape retention (Fig. 6c and d). Therefore, the choice of a suitable debinding support exhibits one way to control the degree of the exudated surface binder film above the melting point of the binder and, thus, the shape retention of the micro parts.

At the initial stage of thermal debinding (70–150 °C) the liquid binder is removed from the green body compact by the interaction of

(i) liquid transport due to the thermal expansion of the binder (exudation effect) [33,34],

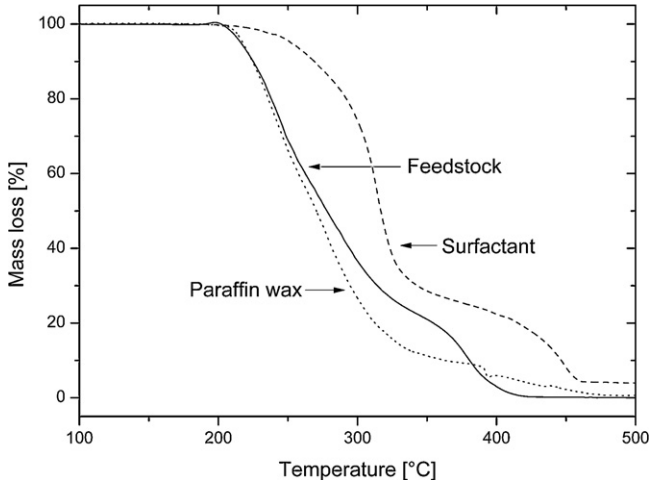

Fig. 7. Thermogravimetric analysis of paraffin wax, surfactant and a feedstock formulation.

(ii) capillary transport to the compact surface by capillary action of the debinding support (or wick) [35,36],
(iii) reduction of the binder viscosity with increasing temperature,
(iv) force of gravity,
(v) interfacial surface tension at the interface binder/debinding support (or wick) [36].

With increasing temperature (above 200 °C) the thermal degradation of the binder becomes effective and starts to prevail as can be seen in the thermogravimetric analysis (Fig. 7). The capillary action of the debinding support (ii) and the interfacial tension at the interface binder/debinding support (v) can be influenced by the type of debinding support. In this study a debinding support with an open porosity of 36% and a mean radius of the open porosity of about 500 nm was used. In comparison, the open porosity of thermally debinded green parts exhibits higher values of around 46% with a mean radius of approximately 60 nm. This means that the capillary action of the debinding support is not pronounced at all. A pronounced surface binder film is formed in the initial stage of thermal debinding, which facilitates the mobility and rearrangement of the particles on the surface of the green parts. Eventually, this results in an improved surface finish as well as edge rounding and, in the worst case, the loss of geometrical integrity (Fig. 6b).

3.3.2. Contact time between feedstock and silicone mould (time for moulding and cooling of mould)

The use of cost-effective and re-usable moulds with high moulding accuracy, e.g. silicone moulds, is one specific feature

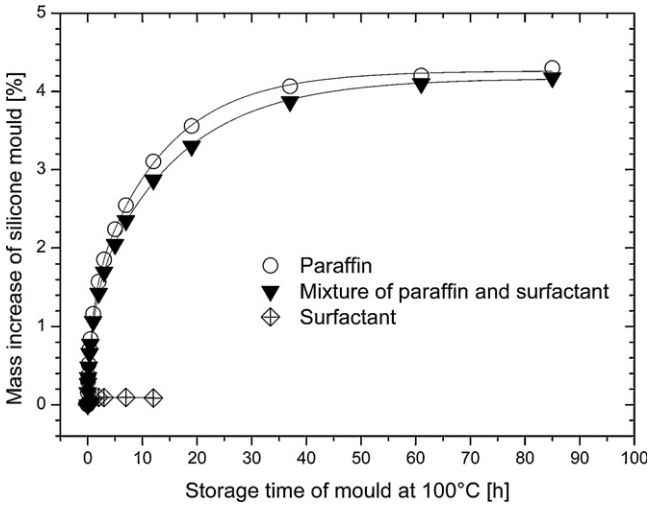

Fig. 8. Time-dependent mass increase of silicone moulds stored at 100 °C in paraffin wax, mixture of paraffin wax and surfactant equivalent to a feedstock formulation with 2.4 mg/m^2 surfactant concentration.

of the RPPC for manufacturing ceramic micro parts via LPIM. However, one major drawback of this process was found to be the absorption of paraffin wax by silicone moulds, which has a significant impact on the shape retention and reproducibility of the micro bending bars during thermal debinding. To determine the extent of absorption capacity, the mass increase of silicone moulds was measured, when stored at 100 °C in paraffin wax and/or surfactant (Fig. 8). A remarkable absorption capacity of silicone for paraffin wax was observed. Saturation with 4.3% and 4.2%, based on the mass of silicone moulds, was observed for paraffin wax and the mixture of paraffin wax and surfactant, respectively. The mass increase of 0.1% was negligible in the case of pure surfactant.

This observation exhibits an important explanation for the poor reproducibility of the shape retention in terms of edge rounding during thermal debinding in the past. In this study, moulds were filled pressureless and manually without using a LPIM machine. Therefore, the moulding time, i.e. filling of the mould and further evacuation, varied often due to the manual procedure. Moreover, during cooling of the moulded feedstock at ambient atmosphere, the contact between feedstock and mould was maintained until the feedstock solidified to a green part. Therefore, special focus was directed at the influence of the total moulding time on the shape retention of the micro bending bars during debinding.

In Fig. 9 micro bending bars after debinding are illustrated at different magnifications. In case of a contact time of only 2 min between the molten feedstock and the silicone mould, an average edge rounding of approximately 12.8 μm was observed (Fig. 9b), whereas in case of 30 min it was not possible to maintain the geometrical integrity of the micro columns during debinding (Fig. 9a). This can be explained by a reduction of the paraffin wax concentration in the micro columns due to the diffusion of the paraffin wax into the silicone mould. As shown in Fig. 8, a considerable amount of paraffin wax can be absorbed by the moulds, whereas the surfactant shows no considerable affinity to silicone. The depletion of paraffin wax results in an increase of the ratio of surfactant concentration in the micro columns, which, in turn, further decreases the yield point of the molten feedstock. Consequently, this weakens the dimensional stability of the micro parts during debinding. For short contact times, e.g. 2 min, the paraffin wax depletion

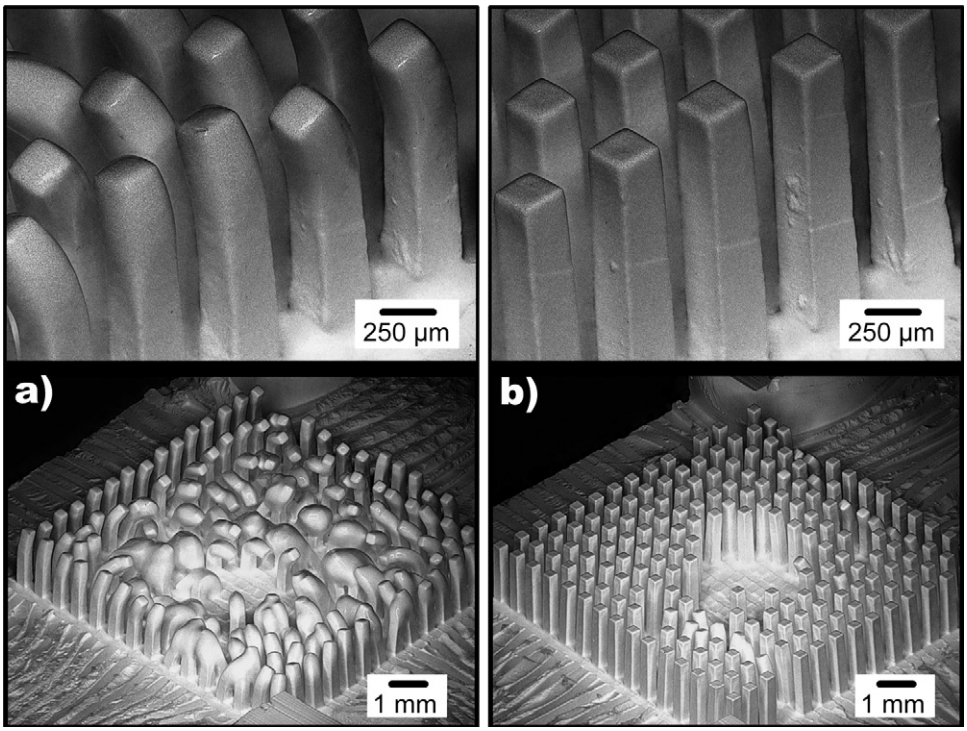

Fig. 9. Debinded green parts fabricated by maintaining a contact time between feedstock and silicone mould of (a) 30 min and (b) 2 min; sample A-S2 (b) exhibits an edge rounding of 12.8 ± 0.6 μm (Table 2), whereas for sample A-S1 (a) it was not possible to maintain geometrical integrity during debinding.

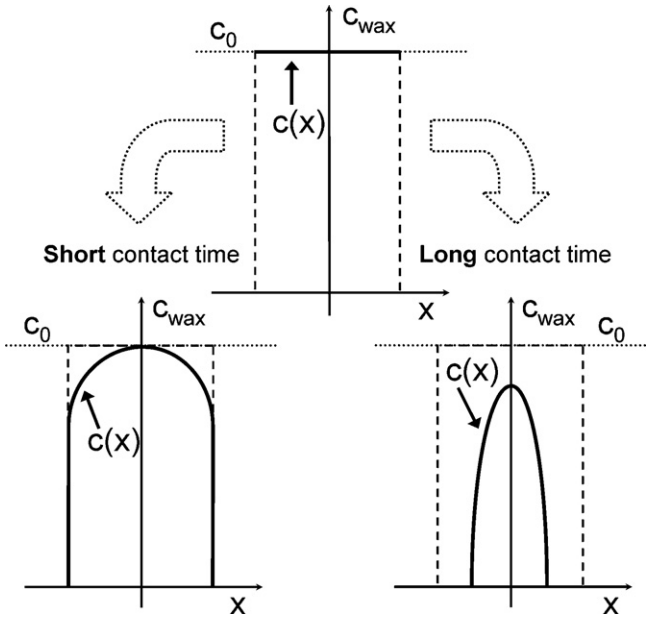

Fig. 10. Schematic distribution of the paraffin wax concentration in a green micro bending bar depending on the total contact time between molten feedstock and silicone mould.

seems to be limited to an area near the surface of the micro columns (Fig. 10) resulting in deformation in terms of edge rounding (Fig. 9b). In contrast, for longer contact times, e.g. 30 min, an increase of the surfactant concentration seems to occur also in surface-off areas (Fig. 10) and, hence, causes deformation (Fig. 9a).

Additionally, the cooling rate of the moulded molten feedstock has to be taken into account. An accelerated cooling of the mould, e.g. quenching in water, led to an edge rounding of 4.7 μm for a feedstock formulation with a surfactant concentration of 3.2 mg/m^2 (A-Q1), whereas for standard cooling rates at ambient air the edge rounding for the same feedstock composition (A-S2) is significantly higher with 12.8 μm (Table 3). Hence, the total time of contact between the molten feedstock and silicone mould, i.e. duration of moulding and cooling of the mould, represents an important process-related impact factor on shape retention, deformation in terms of edge rounding and, altogether, reproducibility of hot moulded ceramic micro parts. In this regard, a pre-treatment of unused silicone moulds in terms of storage in molten paraffin wax for several hours and specified moulding times are proposed to limit the remarkable impact of paraffin wax diffusion into the mould.

3.3.3. Storage condition of green parts: water immersion

Another process-related influencing factor on shape retention of micro parts during thermal debinding was found to be the storage condition of the green parts. When the green parts were directly stored in a dry exsiccator after demoulding or in case of immediate debinding, the edge rounding of micro bending bars turned out to be remarkably higher than in case the green parts were immersed in water for a certain time before debinding. For instance, average edge roundings of 12.8 μm and 4.8 μm were measured for arrays A-S2 and A-S4, respectively, which were debinded immediately after demoulding, whereas values of 5.2 μm and 2.8 μm were obtained for arrays A-W1 and A-W2, respectively, which were immersed in green state in water for 48 h before debinding (Table 3). It is assumed that water diffuses into the green part and causes an increase of the yield point of the feedstock formulation by interfering with the surfactant–powder particle bond and, thus, diminishing the tendency to deformation and edge rounding [37]. It may also be possible that the surfactant concentration in the green part is decreased due to extraction by water. It could be verified that, among several factors, as absorptivity of the debinding support, surfactant concentration, time for moulding and cooling of the mould, the storage conditions of the green parts exhibit another way to control the shape retention and edge rounding of hot moulded ceramic micro parts.

Table 3
Representative samples demonstrating the impact of material and process-related factors on the shape retention of micro bending bars in terms of edge rounding.

Sample	Surfactant concentration (mg/m^2)	Moulding time (min)	Type of cooling[a]	Type of green body storage[b]	Debinding atmosphere[c]	Edge rounding[d] (μm)
A-S1	3.2	30	Standard	–	Ambient air	Deformation
A-S2	3.2	2	Standard	–	Ambient air	12.8 ± 0.6
A-S3	2.8	30	Standard	–	Ambient air	8.0 ± 1.4
A-S4	2.8	2	Standard	–	Ambient air	4.8 ± 0.5
A-Q1	3.2	2	Quenching	–	Ambient air	4.7 ± 0.9
A-Q2	2.8	2	Quenching	–	Ambient air	5.0 ± 1.0
A-W1	3.2	2	Standard	48 h in water	Ambient air	5.2 ± 1.1
A-W2	2.8	2	Standard	48 h in water	Ambient air	2.8 ± 0.5
A-A1	3.2	2	Standard	–	Dry air	3.4 ± 0.5
A-A2	2.8	2	Standard	–	Dry air	2.5 ± 0.4
A-A3	2.8	30	Standard	–	Dry air	3.1 ± 0.4

[a] Standard: cooling down of moulded feedstock and mould at ambient air; quenching: in water (25 °C).
[b] Storage in exsiccator or immediate debinding after moulding.
[c] Ambient air: relative humidity 20–50%; dry air: relative humidity 0%.
[d] Edge rounding of sintered micro bending bars.

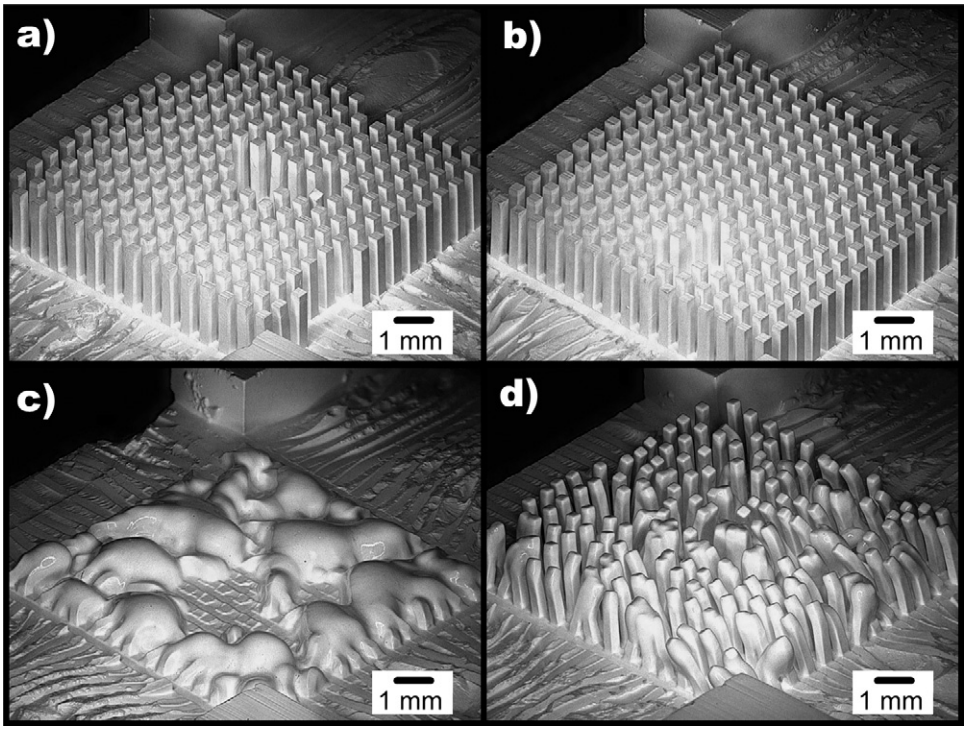

Fig. 11. Debinded green parts with 3.2 mg/m^2 surfactant concentration processed in dry air (a and b) and air with high moisture of about 80–90% (c and d); in (a) and (c) moulding time of 30 min was chosen, whereas 2 min was set in (b) and (d).

3.3.4. Moisture of debinding atmosphere

Besides the process-related influences on shape retention discussed above, the moisture of the debinding atmosphere was found to be a global influencing factor with the highest impact on the geometrical integrity of green micro parts during debinding. Depending on other influences, the debinding at ambient air or intentionally moisturized air caused distinctive edge roundings or total loss of geometrical integrity. In comparison, debinding in dry air usually led to complete shape retention without edge rounding (Fig. 11). For instance, edge rounding of 3.4 μm and 3.1 μm were measured for samples A-A1 and A-A3, respectively, which were debinded in dry air (Table 3). In contrast, samples A-S2 and A-S3, which were debinded as usual at ambient air, exhibited values of 12.8 μm and 8.0 μm, respectively (Table 3). Moreover, complete shape retention was observed for an identical sample to A-S1 (Fig. 9a), when processed in dry air (Fig. 11a).

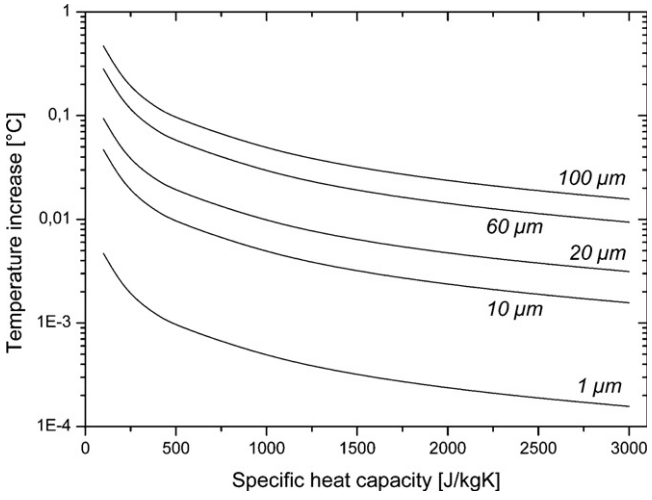

Fig. 12. Calculated temperature increase on the surface of green parts during debinding due to the heat of condensation of water vapour at 100 °C in dependency on the thickness of condensed water.

In a first step it was investigated whether the heat of condensation of water vapour in the debinding atmosphere may cause an increase of the surface temperature of the green parts resulting in the observed tendency to edge rounding or even deformation. Therefore, the theoretical temperature increase ΔT due to the heat of condensation of water vapour during debinding was calculated according to Eq. (5), where ΔH_v and ρ_w are the enthalpy of vapourization and density of water at a specific temperature, respectively, S_g and m_g stand for the surface and mass of the debinded green part, c_P is the specific heat capacity of the green part and h_L stands for the thickness of the condensed water on the sample's surface.

$$\Delta T = \Delta H_v \frac{\rho_w S_g h_L}{c_P m_g} \quad (5)$$

Applying representative values to Eq. (5), a theoretical temperature increase at 100 °C was calculated depending on the heat capacity of the green part and layer thickness of condensed water vapour. In view of an effective specific heat capacity of about 500 J/kg K for ZrO_2 [14] and typical values of 2000–3000 J/kg K for paraffin waxes [38] as well as an supposed layer thickness of condensed water vapour in the range of 1–

100 μm, negligible temperature increases, not higher than 0.1 °C were calculated (Fig. 12). Hence, the assumption of temperature increase due to heat of condensation of water vapour cannot explain the observed tendency to edge rounding and deformation of the micro parts during debinding in ambient air.

It is supposed that a change of the interfacial surface tension at the binder/air interface occurs depending on the moisture content of the debinding atmosphere. As already discussed and shown in Fig. 6, an exudated binder film is formed on the surface of the micro bending bars in the initial stage of thermal debinding. Assuming that the interfacial tension at the binder/air interface is higher for moist air compared to dry air, the tendency to edge rounding and even deformation should be higher in moist than in dry air. A detailed investigation of this topic will be object of a further study.

4. Conclusions

Zirconia (3Y-TZP) micro bending bars with 3-point bending strength up to 2808 MPa and Weibull's modulus of 8–11 were fabricated via hot moulding. The obtained bending strengths considerably exceed values predicted by the Weibull size-scaling effect. A distinctive surface binder film could be observed at the initial stage of thermal debinding, which is responsible for a micro-specific healing and levelling of surface defects, resulting in enhanced surface quality of the micro parts and a reduction of the surface roughness. As the number and size of surface defects decrease, the mechanical properties of the bending bars get improved. It was demonstrated that the size effect is one reason for the high strength values in micro dimension. However, it could be also revealed that the improved surface quality of the micro specimen is the main reason for the very high strength values presented in this study.

Several indicators and process-related factors were found to affect the shape retention and surface quality of green parts during thermal debinding. It was found that an increasing amount of surfactant significantly reduces binder and feedstock viscosity as well as the yield point of feedstocks, resulting in an improved surface finish and, thus, enhanced strength. However, the resistance against deformation is reduced at the same time, which gives rise to edge rounding and, in the worst case, to the loss of geometrical integrity of the micro parts.

The tendency to deformation during debinding was also found to be affected by the absorptivity of the debinding support. Less pronounced capillary action can be achieved using debinding supports with low open porosity and sufficiently large pore size compared to the powder compact.

While the molten feedstock remains in contact with the silicone mould during hot moulding, an enrichment of surfactant occurs in the micro columns due to diffusion of paraffin wax into silicone, which causes a decrease of the yield point. Depending on the contact time, the degree of deformation may vary from edge rounding to total loss of geometrical integrity, as the depletion layer of paraffin wax in the columns varies with time.

Water in terms of a storage medium was found to have a beneficial effect on shape retention. Micro column arrays in the green state, which were immersed in water for a certain time before debinding, exhibited a lower tendency to edge rounding than specimen immediately stored in an exsiccator and directly debinded after demoulding.

By thermal debinding in dry air, complete shape retention could be assured even for feedstocks with high amounts of surfactant, which exhibit the lowest resistance against deformation. In contrary, standard debinding at humid air usually caused deformation. It was deduced that a temperature increase on the surface of the green parts due to the heat of condensation of water vapour cannot be responsible for the deformation tendency during debinding in humid air. Instead, a higher interfacial surface tension at the binder/air interface for humid air compared with dry air is assumed to result in a higher tendency to deformation.

The study reveals that there are several process-related influencing factors on shape retention and surface finish of micro bending bars. Further investigations are needed to reveal additional impact factors and assure a better understanding of the interaction of all influencing parameters that may enable an additional improvement of surface quality and mechanical properties. Considering a decoupling of edge rounding and healing of surface defects, the results of this study exhibit a promising prospect for an easy and reasonable enhancement of mechanical properties of ceramic and metallic micro components fabricated via LPIM. The in-process improvement of the reliability of ceramic micro components without cost-intensive surface post-processing exhibits a remarkable economic potential for μ-PIM.

Acknowledgements

The authors wish to thank Joachim Rögner and Karl-Heinz Lang (Karlsruhe Institute of Technology, IAM-WK) for granting access to the micro 3-point bending device as well as their support in characterization of micro bending strength. Marcus Müller is gratefully acknowledged for his scientific support. The authors also thank Michael Schulz for support on the real-time observations of thermal debinding. Thermogravimetric analyses of Christina Odemer and porosity measurements of Margarete Offermann (all Karlsruhe Institute of Technology, IAM-WPT) are also gratefully acknowledged.

References

[1] H.-J. Ritzhaupt-Kleissl, R.A. Dorey, Ceramics in microtechnology: status requirements and challenges, in: H.-J. Ritzhaupt-Kleissl, P. Johander (Eds.), Ceramics Processing in Microtechnology, Whittles Publishing, Dunbeath, 2009, pp. 1–22.

[2] W. Bauer, R. Knitter, Development of a rapid prototyping process chain for the production of ceramic microcomponents, Journal of Materials Science 37 (2002) 3127–3140.

[3] R.M. German, Medical and dental applications for microminiature powder injection moulding – a roadmap for growth, Powder Injection Moulding International 3 (2) (2009) 21–29.

[4] W. Bauer, R. Knitter, Low-pressure injection moulding, in: H.-J. Ritzhaupt-Kleissl, P. Johander (Eds.), Ceramics Processing in Microtechnology, Whittles Publishing, Dunbeath, 2009, pp. 158–170.
[5] R. Lenk, Hot moulding – an interesting forming process, Ceramic Forum International 72 (10) (1995) 636–639.
[6] V. Piotter, W. Bauer, T. Benzler, A. Emde, Injection molding of components for microsystems, Microsystem Technologies 7 (2001) 99–102.
[7] W. Bauer, J. Hausselt, L. Merz, M. Müller, G. Örlygsson, S. Rath, Microceramic injection molding, in: H. Baltes, O. Brand, G.K. Fedder, C. Hierold, J. Korvink, O. Tabata (Eds.), Microengineering of Metals and Ceramics (Part I), Wiley-VCH, Weinheim, 2005, pp. 325–356.
[8] R. Knitter, W. Bauer, D. Göhring, J. Haußelt, Manufacturing of ceramic microcomponents by a rapid prototyping process chain, Advanced Engineering Materials 3 (1–2) (2001) 49–54.
[9] W. Bauer, M. Müller, R. Knitter, P. Börsting, A. Albers, M. Deuchert, V. Schulze, Design and prototyping of a ceramic micro turbine: a case study, Microsystem Technologies 16 (2010) 607–615.
[10] DIN EN 843-5:2007-03: Advanced Technical Ceramics – Mechanical Properties of Monolithic Ceramics at Room Temperature – Part 5: Statistical Analysis, Berlin, Beuth Verlag, 2007.
[11] M. Auhorn, T. Beck, V. Schulze, D. Löhe, Quasi-static and cyclic testing of specimens with high aspect ratios produced by micro-casting and micro-powder-injection-moulding, Microsystem Technologies 8 (2002) 109–112.
[12] K. Obergfell, T. Beck, V. Schulze, D. Löhe, Construction, controlling and measuring devices of a micro universal tensile test machine, Materialpruefung/Materials Testing 42 (10) (2000) 391–395.
[13] J. Rögner, Mechanische Eigenschaften urgeformter Mikroproben aus $CuAl_{10}Ni_5Fe_4$, ZrO_2 und Si_3N_4, Ph.D. Thesis, Karlsruhe Institute of Technology, Department of Mechanical Engineering, Karlsruhe, 2010.
[14] D. Munz, T. Fett, Ceramics: Mechanical Properties, Failure Behaviour, Materials Selection, Springer, Berlin, 1999.
[15] R.G. Hoagland, C.W. Marschall, W.H. Duckworth, Reduction of errors in ceramic bend tests, Journal of the American Ceramic Society 59 (5–6) (1976) 189–192.
[16] G.N. Doz, J.D. Riera, Influence of support friction on three-point bend test, International Journal of Pressure Vessels and Piping 51 (3) (1992) 373–380.
[17] W. Van Paepegem, K. De Geyter, P. Vanhooymissen, J. Degrieck, Effect of friction on the hysteresis loops from three-point bending fatigue tests of fibre-reinforced composites, Composite Structures 72 (2) (2006) 212–217.
[18] B. Basu, J. Vleugels, O. Van Der Biest, Microstructure–toughness–wear relationship of tetragonal zirconia ceramics, Journal of the European Ceramic Society 24 (7) (2004) 2031–2040.
[19] J. Munoz-Saldana, H. Balmori-Ramirez, D. Jaramillo-Vigueras, G.A. Schneider, Mechanical properties and low-temperature aging of tetragonal zirconia polycrystals processed by hot isostatic pressing, Journal of Materials Research 18 (10) (2003) 2415–2426.
[20] R. Singh, Sintering microstructure and mechanical properties of commercial Y-TZPs, Journal of Materials Science 31 (1996).
[21] DIN 4768: Determination of Surface Roughness Values of the Parameters R_a, R_z, R_{max} by Means of Electrical Contact (Stylus) Instruments, Berlin, Beuth Verlag, 1990.
[22] R. Danzer, T. Lube, P. Supancic, R. Damani, Fracture of ceramics, Advanced Engineering Materials 10 (4) (2008) 275–298.
[23] R. Danzer, P. Supancic, J. Pascual, T. Lube, Fracture statistics of ceramics – Weibull statistics and deviations from Weibull statistics, Engineering Fracture Mechanics 74 (18) (2007) 2919.
[24] G.D. Quinn, R. Morell, Design data for engineering ceramics – a review of the flexure test, Journal of the American Ceramic Society (1991).
[25] W.J. Tseng, M. Taniguchi, T.I. Yamada, Transformation strengthening of as-fired zirconia ceramics, Ceramics International 25 (6) (1999) 545.
[26] G.D. Quinn, Weibull strength scaling for standardized rectangular flexure specimens, Journal of the American Ceramic Society 86 (3) (2003) 508–510.
[27] R. Danzer, Some notes on the correlation between fracture and defect statistics: are Weibull statistics valid for very small specimens? Journal of the European Ceramic Society 26 (15) (2006) 3043–3049.
[28] F.A. Çetinel, M. Müller, J. Rögner, W. Bauer, J. Haußelt, Influence of dispersant on rheology of zirconia–paraffin feedstocks and mechanical properties of micro parts fabricated via LPIM, Ceramic Engineering and Science Proceedings 31 (8) (2010) 31–43.
[29] M. Müller, J. Rögner, B. Okolo, W. Bauer, H.-J. Ritzhaupt-Kleissl, Factors influencing the mechanical properties of moulded zirconia micro parts, in: Proceedings of the 10th International Conference and Exhibition of the European Ceramic Society, Berlin, 2007, pp. 1291–1296.
[30] F.A. Çetinel, W. Bauer, M. Müller, R. Knitter, J. Haußelt, Influence of dispersant, storage time and temperature on the rheological properties of zirconia–paraffin feedstocks for LPIM, Journal of European Ceramic Society 30 (6) (2010) 1391–1400.
[31] R. Finn, Capillary surface interfaces, Notices of the American Mathematical Society 46 (7) (1999) 770–781.
[32] J.H. Song, J.R.G. Evans, Flocculation after injection molding in ceramic suspensions, Journal of Materials Research 9 (9) (1994) 2386–2397.
[33] M.R. Barone, J.C. Ulicny, Liquid-phase transport during removal of organic binders in injection-molded ceramics, Journal of American Ceramic Society 73 (11) (1990) 3323–3333.
[34] L. Gorjan, A. Dakskobler, T. Kosmac, Partial wick-debinding of low-pressure powder injection-moulded ceramic parts, Journal of the European Ceramic Society 30 (2010) 3013–3021.
[35] I.M. Somasundram, A. Cendrowicz, D.I. Wilson, M.L. Johns, Phenomenological study and modelling of wick debinding, Chemical Engineering Science 63 (14) (2008) 3802–3809.
[36] R.M. German, Theory of thermal debinding, International Journal of Powder Metallurgy and Powder Technology 23 (4) (1987) 237–245.
[37] S. Novak, A. Dakskobler, V. Ribitsch, The effect of water on the behaviour of alumina–paraffin suspensions for low-pressure injection moulding (LPIM), Journal of the European Ceramic Society 20 (12) (2000) 2175–2181.
[38] M. Hadjieva, S. Kanev, J. Argirov, Thermophysical properties of some paraffins applicable to thermal energy storage, Solar Energy Materials and Solar Cells 27 (2) (1992) 181–187.